THE

AIR CUSHION TECHNOLOGY PROGRAMME

AT THE

UNIVERSITY OF TORONTO

P. A. Sullivan
Institute for Aerospace Studies

5 May, 1974.

presented at

First International Hovering Craft Conference

Brighton, England

13-16 May, 1974

Abstract

This paper reviews the origins and current objectives of the air cushion technology research programme at the Institute for Aerospace Studies, University of Toronto and discusses some recent research results. Static pitch tests on multicell and an open-loop and finger skirts are presented and the effect of installed power and lift fan characteristic on these are investigated. Some exploratory tests on skirt materials are reviewed, the tests which were considered are tear strength, notching, fatigue, abrasion and dynamic properties. Measurements of external noise generated by an ACV propeller were analyzed by several methods, the data suggested that uneven inflow was increasing noise levels.

Contents

1. INTRODUCTION

1.1 Background
1.2 Current Status of the UTIAS Programme

2. SOME RESULTS FROM THE CUSHION PROPERTIES EVALUATION PROGRAMME

2.1 General Objectives
2.2 Scaling Parameters
2.3 Static Pitch Tests
2.4 Conclusions

3. SKIRT MATERIALS STUDIES

3.1 General Objectives
3.2 Evaluation and Development of Test Techniques
3.3 Constitutive Relations
3.4 Conclusions

4. ROTOR NOISE RESEARCH

4.1 General Objectives
4.2 Some Propeller Noise Measurements
4.3 Discussion and Conclusions

5. ACKNOWLEDGEMENTS

6. REFERENCES

FIGURES

1. INTRODUCTION

1.1 Background

Research at the Institute for Aerospace Studies, University of Toronto (UTIAS) related to air cushion vehicles (ACV) can be traced back to the mid 1950s. In common with much of the early work in Britain, France and the USA, this effort was primarly aimed at understanding the basic aerodynamics of the peripheral jet and other ground effect phenomena (see for example, Refs. 1,2). However, the Institute had developed an active programme in flight dynamics under the direction of Etkin (Ref. 3), and some effort was expended in applying some of this background to the ACV. A feature was the exploration of the usefulness of a circular track facility for the study of the dynamic characteristics of free flight vehicles (Refs. 4,5). Ultimately 15 reports and technical notes were produced from the UTIAS activities, but the work came to a halt by about 1965, mainly because the excessive power requirements and serious control problems of the basic ACV were believed to make it impractical and uneconomic.

The development which reversed this situation was the demonstration of workable flexible skirts by the British and the French, and renewed Canadian interest was followed by a decision in 1969 to reactivate our activities in this area. The new programme differed from the earlier efforts in two essential respects. Firstly, there was a growing awareness that the classical aerodynamically propelled free flight type of ACV, such as the British Hovercraft Corporation's SRN 6, was only one of a number of possible applications, each of which was to some degree controversial, and certainly not yet proven. Secondly, the problem areas which had emerged from earlier experience required research on a much broader front than originally percieved both at UTIAS and elsewhere.

Currently, the major Canadian industrial activities are:

(i) the development of the Bell Voyageur and Viking free flight aerodynamically propelled ACVs.

(ii) use of large air cushion transporters such as the 250 Ton. G.W. ACT-100 for oil rig moves and similar transportation problems in the Arctic.

(iii) application of air cushion trailers such as the 15 Ton payload Terracross H-115 and the Hoverjak HJ-15 in an off road environment.

(iv) applications of air cushions to reduce axle loads on road trailers hauling heavy loads such as transformers, especially during the half-load season*.

(v) exploration of the problems of air cushion landing gear in a joint Canadian/US programme on a 35,000 lb modified de Havilland (Canada) Buffalo.

---

* A characteristically Canadian problem. The ground thaw process in the Spring causes the granular base under a sealed road to become relatively unstable, so that a 50% reduction of allowable axle loads has to be imposed.

There are also a number of efforts to develop small recreational ACVs, but this field remains as controversial as ever. Companies appear and disappear with monotonous regularity, and the designs tend to be underpowered, noisy and uncontrollable. Indeed one jurisdiction (Ontario) has even proposed an outright ban.

1.2 Current Status of the UTIAS Programme

The UTIAS effort is in three major areas: cushion and vehicle dynamics, skirt materials, and noise. With the aid of a Negotiated Development Grant from the National Research Council of Canada, a number of major facilities have been built and are either in operation or nearing completion.

A cushion dynamics rig capable of taking 8 ft x 4 ft models up to 600 lb gross weight is currently being used for static stiffness tests in pitch and roll. (Fig. 1.1). The cushion air supply system includes a flow choke and an infinitely variable speed drive so that both the installed power and the shape of the effective fan characteristic can be varied during a run. In addition to basic pressure and volume flow instrumentation, the data system includes force links, angular and linear displacement transducers and a u/v chart recorder, so that dynamic phenomena can be studied. A servohydraulically driven heave table for simulating long wavelength disturbances has been installed, and a moving belt base for studying the effect of moving over smooth ground is being designed.

A 140 ft diameter enclosed circular test track provides for the logical extension of the work on the cushion dynamics rig. This track, which is enclosed in a 186 ft diameter by 45 ft high geodetic dome, can test models with planforms up to 14 ft by 7 ft. The first test vehicle, Vampire 1, has recently gone up on cushion; in Fig. 1.2 it can be seen in front of the model bay and control room. Our first experiments are planned for the late Summer.

Figure 1.3 is a block diagram of the instrumentation and data acquisition system. Three linear accelerometers and three rate gyros are mounted at the centre of gravity of the vehicle in a thermally controlled oven. Three trailing arms mounted on the sides and back of the vehicle give its height, and roll and pitch angles. A tether tension strain gauge and angular displacement transducer mounted on the tether gimbal system measure the tether constraint force magnitude and direction. A 33-channel slip ring assembly has been installed in the tether centre post to transmit data to the Hewlett Packard HP 2100A data acquisition computer. The computer program converts the analog data to digital form and then stores it on magnetic tape, and allows the operator to specify a sampling rate of 100 times each second for 16 signal channels. A TV camera mounted on the tether post and rotating with the tether transmits its signal through a slip ring to a TV monitor and video tape recorder in the control room for monitoring purposes. In addition, propeller and fan speeds are continuously monitored.

A third major facility, for rotor noise testing relevant to ACVs and other applications, is under construction. It comprises an open jet, open return wind tunnel circuit with an appropriate inlet contraction and special propulsion quieting. The test section, which has a diameter of 3 ft., is open to a large anechoic volume completely surrounding the test area, permitting acoustic measurements of the free field type exterior to the air flow. The dome covering the circular track is used as a large plenum of turbulence-free air, which is ultimately discharged to atmosphere through an axial flow fan stage. The total installed power is 150 hp, while the cutoff frequency of the anechoic measurement area is 160 hz. Maximum test section velocities expected are in the order of 300 ft/sec.

Two modes of operation for fan and rotor noise measurements are envisaged with this facility: a static mode and a simulated forward velocity mode. In the former mode, the fan unit is operated in the anechoic chamber, without test section, and with the front wall of the facility opened by means of several full height slots located ahead of the anechoic lining. In the forward velocity mode the test section is utilized with the model air flow induced by the downstream fan. In this condition the slotted wall openings are covered and the inlet contraction cone substituted upstream. A scaled drawing of this facility is shown in Fig. 1.4.

Although our facilities are not yet all operational, some aspects of our programme have been producing data, and the remainder of the paper describes some of these results.

2. SOME RESULTS FROM THE CUSHION PROPERTIES EVALUATION PROGRAMME

2.1 General Objectives

The primary objective of this programme, which is being undertaken on the cushion dynamics facility, is to obtain data on some representative flexible skirt systems, both to assist the designer and to provide a basis for development of alternative designs. It is interesting to note in this respect that, although considerable effort has been expended in the exploration of skirt designs available to date, there does not appear to exist in open literature details of the properties of skirt systems comparable to the information available on fans or airfoils. Furthermore, the need for improvements on existing designs is especially apparent in Canada,has recently been emphasized by the trials of trailers in Rageneu, Quebec (Ref.14, p.29). This is not unreasonable since, although the developments in Europe have made considerable advances, they have primarily been concentrated on overwater applications in essentially temperate climates, whereas the Canadian experience relates more to overland and the Arctic operations.

Currently tests are underway on the static pitch and roll stiffnesses of two generic skirt systems:

(i) a resistance orifice fed multicell system reminiscent of Bertin designs,

(ii) an open loop and finger system related to HDL designs.

Some of the initial data on pitch tests will be presented in Section 2.3.

2.2 Scaling Parameters

(i) Basic Approach: - In order to present the data in a way which is useful for scaling to full size designs it is essential to use nondimensional parameter groups. Often the choice of appropriate groups is guided by a theory, but in the case of cushion systems, because very little in the way of unified theories exist, one cannot go much beyond the purely mathematical exercise of using the Π theorem. This is due in part to the geometrical complexity of the cushion and their aerodynamic duct feeding systems. In general, the following approach seems to be emerging. For a given class of application, cushion design or geometry, and gross vehicle weight W, the mean or nominal cushion pressure p_c is dictated largely by practical considerations such as cargo density, allowable vehicle width associated with road restrictions, and the like. Hence the planform area A can be regarded as an independent variable and $p_c = k\ W/A$, where k is a coefficient determined entirely by the geometry of the deployed skirt. Usually k is slightly greater than unity. The three remaining choices are the cushion air equilibrium mass flow, the local slope of the pressure-mass flow characteristic of the air supply system, and the skirt material. As a rough guideline the cushion flow will be determined by the dynamics of the interaction of the particular vehicle and its operating environment, while the choice skirt material will be selected almost entirely by questions of cost, manufacturing ease, and longevity.

(ii) Scaling Cushion Flow: - Trillo (Ref. 6,p.32) suggests a cushion flow coefficient C_{QC} given by

$$C_{QC} = \frac{Q_e}{v_{ref} A_{ref}}$$

where Q_e is the cushion equilibrium air flow, A is a reference area which is usually taken to be either the cushion "foot print" area A_p or the base area of the hard structure A_b, and v_{ref} is a suitable reference speed. The natural choice of v_{ref} is the cushion air escape speed based on the Bernoulli law, that is $v_{ref} = \sqrt{2p_c/\rho_c}$, where ρ_c is the cushion air density.

Hence

$$C_{QC} = \frac{Q}{A_{ref}} \sqrt{\frac{\rho_c}{2p_c}}$$

In general, as Trillo points out, the choice of C_{QC} will depend on the environment (marine or land), the craft speed, and suitable statistical measures of surface roughness. For a given operating condition, decreasing C_{QC} will increase the probability of plough-in, or its overland equivalent, hard structure-ground contact.

The author prefers a slightly different approach which is in principle, more general. An alternative choice to the cushion air volume flow Q_e is the equivalent power of the cushion system and, for a designers viewpoint, the interesting parameter is the power-to-weight ratio P/W. Here the estimate of fluid power is taken downstream of the fan system but upstream of any ducting which is intrinsic to the particular design. The latter distinction is crucial since some systems, such as the multicell device used in the present tests, may depend on lossy orifices or other duct work for their basic action. Hence, since $P = Q_e p_{tse}$, where p_{tse} is the equilibrium supply total pressure, a nondimensional cushion power coefficient can be obtained by using a reference velocity related to that suggested by Trillo, $v_{ref} = \sqrt{2p_{ref}/\rho_c}$ with $p_{ref} = W/A_{ref}$

$$C_{PC} = \frac{Q_e\, p_{tse}}{W} \sqrt{\frac{\rho_c\, A_{ref}}{2W}} = \frac{Q_e\, p_{tse}}{W^{3/2}} \sqrt{\frac{A\ \rho_c}{2}}$$

It should be noted that the two coefficients C_{QC} and C_{PC} are closely related. If, as for the open loop and finger system tested here, we can take $p_{tse} \sim p_c$ and the reference area A is chosen so that $W = p_c A$, then $C_{FC} = C_{PC}$.

(iii) Effect of Fan Characteristic: - The other parameter required is the slope of the characteristic of the fan and duct system that supplies the cushion, i.e., dp_s/dQ. Suitable nondimensional forms are

$$C_{SCA} = \frac{Q_e}{p_{tse}} \left.\frac{dp_s}{dQ}\right|_e \quad \text{or} \quad C_{SCB} = A\sqrt{\frac{2A}{\rho_c W}} \left.\frac{dp_s}{dQ}\right|_e$$

where the subscript "e" refers to the nominal operating condition. We have

$$C_{SCB} = (C_T^2/C_{PC})\ C_{SCA}$$

where C_{TC} is another (dependent) grouping given by $C_{TC} = p_{tse}A/W$.

(iv) Limitations: - The idea that the choice of skirt material does not affect the basic vehicle dynamics - implicit in the argument given above - is a very useful simplification, and for many features of ACV behaviour it should be very good indeed. The ratio of cushion pressure to skirt weight per unit area is usually very high, typically of the order of 50:1 to 100:1. Hence for vehicle dominated skirt motions, it is hard to see now a skirt can differ much from a weightless membrane. However, this is not to say that skirt inertial and structural properties are not important; for example they are intrinsic to self excited skirt oscillations, and under some circumstances these can couple with vehicle motion, or induce rapid wear. Also under some circumstances, if the vehicle motion is large enough, not just the local slope of the fan characteristic, but its entire shape may be important. This occurs as the vehicle goes up on cushion. But, at least for examining the dynamic behaviour while on cushion, the effect of local slope should be explored before proceeding to additional complications.

2.3 Static Pitch Tests

(i) General Comments: - As noted earlier, a characteristic feature of this aspect of the ACV field has been the extent of controversy about skirt behaviour coupled with the lack of suitable data. Consequently our first tests were regarded as simply to provide some insight into the parameters which may be important, and into possible basis for theoretical models. It was fully expected that having the data and compared it with suitable mathematical models, we would return to our experiments to define more clearly the effect of the various parameters under the control of the designer.

Our choice of models to examine was not made on any such simplistic basis as attempting to define a "best" commercial design. Apart from the fact the definition of "best" will be different for different applications, we were more interested in choosing designs which encompassed the major ideas implicit in the practical designs available to date. From this view the HDL and Bertin/SEDAM designs seemed to be the furthest apart, with the BHC bag and finger system somewhere in between (Ref. 15).

The curves to be presented were obtained on a rig which was free to move simultaneously in heave and pitch, but constrained from any lateral motion. The axis of rotation was fixed relative to the model and aligned closely with its centre of mass. As can be seen in Figure 1.1, the "model" was an 8 ft x 4 ft box supplied with cushion air through a very soft flexible duct. The box acted as a plenum chamber or reservoir for supplying the cushion system, so that the mean static box pressure and its variation with cushion air volume flow provided the information required for both the effective cushion power C_{PC} and characteristic slope. C_{SC}.

The data was obtained by moving a known test weight along the top of the model on a cart, so that during the individual experiment the total weight remained constant, and the effect of the test weight motion was the same as imposing a pure pitch moment about the model rotation axis. The centre of pressure shift given has been computed relative to the centre of mass of the model, by assuming that the aggregate force provided by the cushion was normal to the smooth horizontal surface on which it was tested. Two potential sources of error in this approximation were considered to be small enough to be ignored. First, the momentum of the escaping air from a pitch or rolled cushion can provide an additional moment owing to the asymmetric outflow. Some order of magnitude computations indicated that for the pitch tests, this effect was negligible, although for roll tests, it might be as much as 10% in some high flow cases. The second potential source of errors related to the frictional forces generated by any portion of the skirt contacting the ground as the vehicle rotated. A simple test was conducted to evaluate this effect for both skirt systems. With the model pitched at an angle such that significant amounts of skirt contact occurred, a thin board was pushed between the skirt and the ground board from both "pitch up" and "pitch down" ends of the model. Any changes in pitch angle between these two actions were noted; in general they were found to be small, provided that the cushion rig was not near a point of static instability.

As noted above the data for the present tests has been given relative to the centre of mass of the vehicle, so that it represents the true restoring moment for this particular "vehicle". However inasmuch as the location of the centre of mass is a function of a particular vehicle, and it is desirable to present the data in a way which is as independent as possible of ancilliary factors, it would be desirable to choose a suitable universal reference plane. The plane containing the lowest point of the hard structure has been suggested for this purpose. This was not done for the present exercise however which was exploratory in nature. It is especially important that this distinction be made for roll tests, where the angles involved are approximately double that obtained in pitch.

The open loop and finger cushion tested here used 90° fingers whose nominal length f was 0.208 of cushion beam. The capabilities built into the cushion system for geometry variation included

(i) internal flow distribution,
(ii) finger attachment distance,
(iii) bag length,

The latter items are defined in Figure 2.1. The effect of internal flow distribution was examined briefly. The cushion air was both dumped directly into the cushion and directed into the loops. Also the distribution of areas was varied; typically the effect of dumping all the air into one end was examined. The results showed only a very small effect on a typical pitch curve.

The multicell skirt tested here has a configuration as shown in Figure 2.3. A total of eight "jupes" or cells were surrounded by an outer skirt which in turn was held laterally by three membranes. Regulation holes fed air both into the cells and into the outer cushion as shown. Each cell had a total of eight small and one large hole each of which could be closed off. Each outer cell had a total of four feed holes. For estimating regulation effects, the reference area per cell was taken to be the total area of the eight small inner feed holes; this reference area was 14.7% of the jupe area. The inner and outer

skirts had the same basic height in contrast to those used on SEDAM craft (Ref. 6, p.91). The origin of this choice lies in the belief that, for overland operations, skirt wear rapidly eliminates any difference.

We found that the test results were very repeatable, although they showed sensitivity to small changes in the skirt geometry. For example, when any curve of centre of pressure (c.p.) shift as a function of pitch angle α, was found to change when a test was repeated, such a change invariably occurred only when there had been a local failure in one of the skirt seams or joints. In general the scatter of the data was small, usually less than $\pm$ 2%.

(ii) Loop and Finger Skirt: Effect of Geometry Changes: - Figure 2.1 compares the effect of changes of loop and finger attachment lengths on the characteristic of the loop and finger start. For the three cases presented the coefficients C_{PC} and C_{SC} were* nominally the same. All three curves showed some hysteresis, with the upper branch corresponding to increasing pitch angle. The slopes of the three curves were virtually identical at about 1% per degree, and the only effect of the geometry changes was to change the equilibrium hoverheight and the maximum pitch angle and CP shift. No doubt these differences can be interpreted entirely in terms of the geometry of the deployed skirt, although the hysteresis is not so easily explained.

(iii) Effect of Power Change on Loop and Finger Skirt: - Figure 2.2 shows the effect of increasing the power to weight ratio by about two, and the major effect is an increase in the maximum roll angle. Since for this cushion system, the supply box pressure was indistinguishable from that measured on the ground board, the predominant effect of an increase in C_{PC} or HP/W is to increase the equilibrium hoverheight somewhat to accomodate the associated increase in cushion flow. Also the sensitivity of the cushion to venting is reduced. This point is discussed below. In general our tests of the loop and finger system support the basic idea that the skirt obtains its action through shift of a constant pressure area relative to the base of the vehicle through skirt deformation associated with cushion-surface contact.

(iv) Multicell Skirt: Effect of Regulating Hole Size: - Figure 2.3 shows typical results for the multicell skirt. All curves show a characteristic break region at which the slope is suddenly reduced; and the return portion shows hysteresis effects. The explanation of this behaviour is reasonably straightforward. The skirt action can be considered to comprise three distinct phases. In the initial steep-slope phase, which may be called the regulating zone, there is no skirt-ground contact. The variation individual of cell clearances causes a corresponding variation in volume flows and associated pressure changes across the regulating holes so that the pressures in cells with reduced gap height increase and vice versa. At about 1 degree skirt-ground contact commences and gradually the entire front pair of cells and then the inner pair are shut off. This may be called the transition zone. The second slope, which occurs in the "shut off" zone, is much less than the first because the cells have entirely lost their regulating ability and are relying on the area changes associated with the slight taper required to obtain a stable shape. Presumably, the hysteresis is associated with redeployment of the jupe acting as a buckled air supported column.

---

* The negative sign in C_{SC} associated with the decreasing pressure-volume flow characteristic required for stability has been omitted.

The comparison in Figure 2.3 provides some support for this argument, since the lower curve, which has the larger feed area, also has reduced slope in the regulating zone. However it is not entirely satisfactory, since both systems have the same C_{PC}, and it is to be expected that the increased stiffness obtained through the use of lossier orifices should be associated with a performance penalty. Specifically, since the equilibrium cell pressure is decided by weight and geometry, for two systems identical in all respects except feed hole size, the one with smaller feeding orifices should have a higher box pressure and lower volume flow for the same C_{PC}. This implies that the onset of the shut-off zone should begin at a smaller angle for the stiffer system. This does not occur here.

The resolution of this difficulty may lie in the differences in the cell feeding arrangements. In a detailed investigation of a circular rigid walled plenum chamber, set up in our laboratory to specifically investigate feeding effects, Rubinstein (Ref. 16) has shown that for a given total feed area, the number of holes and the way in which they were distributed strongly affected lift. The catastrophic lift loss associated with the vortex created by a single large central feed hole has long been known, but even when the number of holes was less than about six significant effects were observed. For the present tests, the increased regulating area was obtained by opening up the large central feed holes. These tests are to be repeated, but keeping the same number of feed holes and varying their size.

(iii) Multicell Skirt: Effect of C_{PC} and C_{SC} Changes: - Figure 2.4 shows the results of three tests, each with values of C_{PC} and C_{SC} chosen to illustrate as closely as possible the effect of changes of one these parameters while holding the other nearly constant. The skirt and feeding geometry was the same for the three curves. With case A taken as the reference, Case B corresponds to a large decrease in fan slope coefficient C_{SC}, while case C corresponds to a large decrease in power coefficient C_{PC}.

Both of the effects seem reasonable in the light of the expected behaviour of this system: a large increase in the (negative) slope of the supply characteristic associated with C_{SC} changing from 4.11 to 7.77 can be expected to cause earlier onset of the shutoff zone. As the cushion pitches and venting occurs at the pitched-up end, one fed by a supply with a steeper characteristic has to move a greater distance in heave in order to shut off flow area and thus recover the pressure required to support the cushion. However, this effect should not be as marked as for a cushion in which the equilibrium Q and thus C_{PC} is reduced, and this seems to be the case here. Note that all three curves show the same slope in the regulating zone.

These results also show the importance of using nondimensional coefficients in analyzing data. Curves B and C correspond to power to weight ratios of 12.9 and 11.9 HP/ton respectively so that there is only a modest difference in this dimensional quantity, but there is a large change in C_{SC} between them. One might be tempted to conclude that this therefore illustrates the effect of change of C_{SC}; however there is also a large change in C_{PC} so that the conclusion that there is a large effect of fan slope is spurious.

(iv) A Comparison Between the Two Systems: - Figure 2.5 compares tests for a multicell and open loop-finger system for values of C_{SC} and C_{PC} as close as were obtained. Both the c.p. shift and the mean cushion height are given as functions of

pitch angle. The differences between the shapes of the two systems are striking, but there are important similarities. There is not much difference between the values of the maximum c.p. shift that the two systems can tolerate and the change in mean or heave height follows almost identical curves for the two systems.

The coupling that occurs between heave and pitch as a direct result of cushion venting is very strongly dependent on both C_{PC} and C_{SC}, as might be expected. For the data given in Figure 2.4, the height change fraction $\Delta h/he$ at maximum pitch for cases A and B were 14.6% and 31.8% respectively (C_{SC} change): while for case C $\Delta h/he$ was 37.6% (C_{PC} change). The coupling is also noticeable in any dynamic motions, with the heave frequency being exactly twice the pitch frequency owing to the fore-aft symmetry of the cushion.

2.4 Concluding Remarks

The results presented above, although encouraging, are only a very modest start. Much more data has to be collected and analyzed in order to confirm the utility of the approach adopted. For example, our current plans call for more detailed exploration of the effect of the fan characteristic by controlling it more closely through the use of an infinitely variable speed drive, for examination of the effects of forward motion and other relevant variables. A similar approach will be adopted for damping effects, coupling between pitch heave and roll, and other motions.

3. SKIRT MATERIALS STUDIES

3.1 General Objectives

As for the cushion studies, this area is characterized by the almost total lack of open technical literature correlating operating experience with laboratory tests. Indeed, as Trillo (Ref. 6, p.51) has stated, until recently there was a reluctance to conduct laboratory tests on the grounds that the results so obtained could not provide the required answers. Fortunately the need for this has now been widely recognized but to date little real progress seems to have been made. We have found it necessary to start from the elementary notion of defining suitable tests and to manufacture test specimens in order to adequately control properties. It seems that the industrial technology of fibre/elastomer composites has not yet progressed to the point where specimens having well defined properties are available on much the same basis as for metals or plastics. In general the elastomer and fabric combination used for skirts is highly anisotropic and may also show strain rate dependence effects, so that apart from the problem of defining the operating environment, it is a relatively complex material to specify.

The UTIAS programme involves two distinct objectives: developing an understanding of the stresses that may occur in skirts for particular classes of design and operation, and understanding the effects of skirt wear. The test programme currently underway has two major components:

(i) (a) the evaluation and development of testing techniques suited to typical skirt materials.

(b) this is to be followed by compilation of data on materials currently in use and the correlation of these test results with field experience.

(ii) Development of mathematical models which are reasonably simple, but which are comprehensive enough to enable effective stressing of skirt elements.

Both programmes use skirt materials and our own laboratory manufactured composites as samples. Phase (a) of the first objectives is well under way, and some of the principal results available will be described below. The tests which have been investigated for suitability are: tensile strength, abrasion resistance, fatigue, tear strength and strain rate effects on Young's modulus. Objective (ii) is proceeding and the techniques currently being explored are briefly reviewed.

The results described below have been presented by Buckley et al (Ref.8) in more detail at the recent Conference on Stresses and Strains in Textile Structures held at the Shirley Institute (U.K.)

3.2 Evaluation and Development of Test Techniques

(i) Tensile Strength and Notches: - Owing to the interaction of the fibres and matrix of a skirt material, several parameters are required to properly characterize its strength. However, simple flat tensile test specimens can be employed to obtain the unidirectional strengths in the major and minor fibre axis directions and,

although such data is of limited use, it does provide a comparative basis for assessing the effects of composition, discontinuities such as cutouts, notches and tears, and residual strength after exposure to abrasion and other hostile environments.

In our notch tests, a number of two-inch wide coupons were prepared, each with a pair of symmetrically placed notches, such that a one-inch wide section was left in the middle of the coupon. The tensile breaking strength of these samples was then compared to that of an un-notched one-inch wide coupon. The results are shown in Fig. 3.1. The interesting feature is that silicone rubber/fibreglass material was virtually unaffected by the presence of the notches, in contrast to the Goodrich material. The latter was taken from an in-service ACV, and is a nylon fabric with a nitrile rubber matrix. The difference is probably due to the relatively higher load carrying capacity of the nitrile rubber matrix compared to that of the silicone rubber. Hence the effect of the notches or cutouts is to produce stress concentrations that reduce the strength of the matrix but not substantially that of the fibres. The data of Fig. 3.1 further supports this view, in that the shape of the notch has a significant effect on the nitrile/nylon material with the trend typical of stress concentrations; whereas the silicone rubber/fibreglass results show only experimental scatter with no trend due to the small contribution made by this matrix to the overall strength.

(ii) Effect of Fatigue on Tensile Strength: - Our initial look at fatigue properties was intended to determine if this could be a major problem in skirt design. Test conditions were selected on the basis of strain measurements made on a Bell Aerospace (Canada) Voyageur type ACV. The selected conditions were considered to be sufficiently beyond the normal operating state that if fatigue effects appeared to be minimal, then one would feel confident in discontinuing further examination.

Nominal one-inch wide coupons of the Goodrich Z9761 material were placed in a SATEC fatigue machine and subjected to a load of 150 lbs. $\pm$ 50 lbs. at 30 cps. This corresponds to a mean 1765 psi ($\sim$ 23% ultimate) and a maximum strain and strain rate of about 20% and 10 sec^{-1}, respectively. The coupons were removed from the machine at arbitrary time intervals and tested to determine their residual tensile strengths. Results obtained so far indicate a minimal fatigue problem. There was less than a 10% decrease in the tensile strength for up to 15 million cycles - longer than the expected life of a skirt component.

(iii) Tear Strength: - Initially, the ASTM standard test D751 (Bird Wing test, Ref. 10), was tried in order to evaluate tear strength. In this method, a three-inch wide coupon eight inches in length containing an initial three-inch slice is fabricated as shown in Fig. 3.2. The two ends of the specimen are then placed in a tensile test machine, and the maximum load required to propagate the cut an additional three inches is noted. Several tests were also conducted to determine the effect of rip-stop holes. The results of these tests, as shown in Fig. 3.2 are somewhat inconclusive. In most cases, a maximum load of 85 to 90 lbs. was observed, regardless of the fabric axis or the size of the rip-stop hole. Once the tear was initiated, the load needed to continue it was about 55 lbs.

The poor results of this test led us then to develop an alternate technicuq. In the one finally chosen, a knife edge is initially impressed into the material, after which a double chamber gas gun is used to fire a projectile, which then impacts a bar to which the knife edge is attached. The distance that the knife edge is driven through the material for a given firing pressure can be used for qualitative comparisons of tear strength with other materials.

UTIAS Reference	AR 1	AR 2	AR 3	UR 1
Manufacturer's Reference	4277.114HB	4278.137HB	4275.320HB	Fiberthin 132
Colour	Black	Black	Black	White/Grey
Coating	Polychloroprene blend	Polychloroprene blend	Polychloroprene blend	Hypalon
Fabric	Nylon ("low-strength")	Nylon	Nylon	Nylon No.1130
t_o (in.)	.045	.054	.126	.0195 $\pm$ .0005
t_e (in.)	0.009	0.004	0.024	0.0005*
P_o(lb./in.)	350 (min)	450 (min)	800 (min)	300
w (oz./sq.yd.)	35	43	100	14 $\pm$ 1

* difficult to determine owing to small value

TABLE 3.1: BASIC DATA OF SKIRT MATERIALS SUBJECTED TO ABRASION TESTING

Some of the initial results are presented in Figure 3.2, and in contrast to the birds wing test, there appears to be excellent repeatability.

(iv) Abrasion Resistance: - Although some significant advances have been made in prolonging the life of marine hovercraft skirts (Ref. 6), little attention has been paid specifically to abrasion effects. It is envisaged that a characteristic feature of Canadian ACV activities will be extensive overland operations, so that it was felt that methods for testing abrasion resistance of skirt materials should be explored. In this context, it should be noted that there does not appear to be any standard tests for this property (Ref. 10) so that we decided upon some simple exploratory studies as a first step.

The standardized conditions of our laboratory tests were chosen to produce a convenient and hopefully repeatable test, rather than to simulate actual operating conditions. The apparatus consisted of a circular cylindrical drum of 7 ins. radius with abrasive surfaces attached. Each specimen was maintained in contact with the abrading surface over a given arc length by a dead weight attached to its lower end, so that it was subject to the same contact pressure. A nominal rotational speed of 610 rpm was chosen. The extent of the abrasion was measured by profiling the surface of each specimen. To this end, the specimen was held flat on a vacuum plate and traversed along its length, at several intervals across its width, by a linear transducer. This was also checked against the mass loss by direct weighing. The tensile strength of the material was also determined before and after the tests, and in this connection it was found that the method prescribed by ASTM (Ref. 10) was not satisfactory, so that it had to be modified (Ref. 11).

The procedure has encountered problems, some of which have been circumvented, and although improvements are desirable, the results are encouraging. After as little as 30 seconds of abrasion, melting of the elastomeric coating occurred. This caused failure of the test, since the increased drag associated with the presence of the plasticized rubber caused the specimen to snatch and jump off the drum. Reduction of the loading weight and drum rotating speed did not alleviate the problem. This had to be circumvented by periodically stopping the test and removing any accumulated rubber. The type of abrasive initially used, which was aluminum oxide, also tended to clog. Silicon carbide was tried and found to be a considerable improvement, although it behaved in a way which suggested that it rapidly lost sharpness.

Some of the data obtained to date is presented in Figs. 3.3 and 3.4. The basic properties of the four specimens examined are given in Table 3.1. The first three samples have been supplied by the Avon Rubber Company, U.K., while the fourth was supplied by Jones, Kirwan & Associates, Canada. Figure 3.3 shows some absolute data for abraded thickness as a function of test time (T hrs) and the age of the abrading surface at the start of the test (S hrs). The results, when plotted on a mass basis show similar trends, and it would seem that those results for $S \simeq 4$ hrs or less are the more useful.

Since the amount of elastomer that is used to coat the fabric is in principle arbitrary, comparison of the amount abraded on an absolute basis is a measure of abrasion resistance. The test therefore suggests that the UR1 material shows the best abrasion resistance, with the AR3 material showing the most wear. This conclusion is supported by the residual tensile strength ratio P_a/P_o as a function of the fraction abraded d/t_o shown in Fig. 3.4. The band drawn in Fig. 3.4 contains

85% of all test results, and it indicates that little strength is lost until the fibres are exposed, after which very rapid deterioration occurs. For the data in Fig. 3.3 with S = 0, the sample UR1 was at a value of $d/t_o < 0.01$ when tested in tension, while the AR3 sample was at $d/t_o \sim 0.2$ when tested.

Consideration is currently being given to redesign of the rig to eliminate the difficulties encountered. Following upon this, the effect of a number of environmental factors will be explored.

(v) Dynamic Properties: - Our investigation of dynamic properties was limited to strain rate effects. In order to achieve high strain rates ($d\epsilon/dt = 10^2 sec^{-1}$), the dynamic load apparatus, detailed in Fig. 3.5 was built for axial straining of flat specimens. The loading rate is determined by the pressure difference across the piston and the orifice size of the main vent. The load washer and the LVDT outputs are recorded on an oscilloscope, giving time histories of the applied load and the axial extension of the specimen. Hence an average Young's Modulus can be obtained for each test specimen at various strain rates. Thus far, two materials have been tested - the B. F. Goodrich Z9761 and the SRN-5 finger material (see Fig. 3.6). The strain rate effect for both coated fabrics is very similar since both materials are nitrile rubber/nylon composites. The Young's Modulus varies over a range of one order of magnitude as the strain rate increases from "static" to about 5 $seconds^{-1}$.

However, it is not yet clear to what extent visco-elastic effects are of practical importance. Measurements of strain and strain rates on the Bell Voyageur bag indicated a maximum strain rate $d\epsilon/dt$ of about .03 sec^{-1}, which suggests that the effect is only marginal. More exploration of this effect is required, since the dynamic strains encountered in a skirt system are superimposed on a mean loading level, and it is thought that the presence of a nonzero mean strain may lower the value of $d\epsilon/dt$ at which significant effects are observed (Ref. 12).

3.3 Constitutive Relations

This part of the programme is aimed at determining the two-dimensional mechanical property coefficients of a coated fabric. The generalized two-dimensional form of Hooke's Law is given by (Ref. 9)

$$\begin{bmatrix} \epsilon_w \\ \epsilon_f \\ \gamma \end{bmatrix} = \begin{bmatrix} E_w^{-1} & -\mu_{wf}E_f^{-1} & \eta_{wwf}G^{-1} \\ -\mu_{fw}E_w^{-1} & E_f^{-1} & \eta_{fwf}G^{-1} \\ \eta_{wfw}E_w^{-1} & \eta_{wff}E_f^{-1} & G^{-1} \end{bmatrix} \begin{bmatrix} \sigma_w \\ \sigma_f \\ \tau \end{bmatrix}$$

which, if applied to coated fabrics, requires a linear relation between stress and strain. There are nine unknown coefficients to be determined. The Young's Modulus for the warp and fill directions (E_w and E_f), the shear modulus (G), the Poisson Ratios relating contraction in the warp direction due to strain in the fill direction (μ_{wf}) and vice versa (μ_{fw}) can be considered as conventional coefficients. The remaining four coefficients can be important in the case of anisotropic coated fabrics. They are identified as coefficients of interaction of the first kind ($\eta_{wf,w}$ and $\eta_{wf,f}$) and of the second kind ($\eta_{w,wf}$ and $\eta_{f,wf}$). These

coefficients relate shear strain to extensional strain (the first kind), and extensional strain to shear strain (the second kind). Since the straining of a coated fabric is not necessarily conservative, all nine coefficients are independent, and multi-valued. The classic linear isotropic material such as a metal requires only two coefficients, say E and Poissons ratio μ. One can easily appreciate that an anisotropic, non-conservative constitute relation of such complexity is impractical from an engineer's point of view. As a result, our programme is aimed at determining strain levels for which less complex models will provide an adequate engineering description of material behaviour.

The technique adopted was to investigate the strain of cylindrical specimens under simultaneous loading in axial tension, torsion and internal pressure. The advantages associated with the use of cylindrical specimens are that it eliminates edge effects and provides a neat way of applying shear and transverse loading (see Fig. 3.7). The material currently being used for exploratory purposes has a polyurethane rubber/fibreglass composition.

Strain data is obtained from each test as follows:

(i) axial strain - dial gauge and photographs of surface grid distortion,

(ii) shear strain - photographs of surface grid distortion,

(iii) circumferential (hoop) strain - Fotonic (non-contacting) optical sensor and low pressure contacting LVDT's.

To date, efforts have been primarily directed towards developing reliable techniques for measuring strain, as this has been the major problem thus far encountered. Figure 3.8 illustrates the difficulty associated with measurements of hoop strain in a simple internal pressure tests. In general, when working with these materials, difficulties in gripping the specimen, the inability to use the classic strain gauge and the like indicate the importance of avoiding reliance on single measurements for obtaining data.

We are currently exploring techniques for eliminating these problems. Some progress has been made; for example, it is believed that the large scatter originally encountered in the photographic measurements can be greatly reduced by the use of a recently introduced high resolution film (Kodak SO-410). It is too early to make any definitive comments but, initial results indicate that these materials are highly anisotropic, with a Young's Modulus ratio of the order of 2 to 1 in the warp and fill directions respectively.

3.4 Conclusions

Although much remains to be done in this area, some useful guidelines can be drawn from our experience to date:

(i) Although the typical skirt material appears to be highly anisotropic, the simple tensile test is useful in establishing effects of such important factors as notching and abrasion.

(ii) The tear resistance technique tried here seems a considerable improvement over the classic Birdswing test.

(iii) Fatigue does not seem to be a significant factor.

(iv) Skirt materials can be highly viscoelastic with the Young's Modulus varying by as much as an order of magnitude. In practical terms this effect is probably not important for vehicle dominated skirt motion, but it certainly could be important for self-excited oscillations such as skirt "buzz", since these can be of very high frequency.

(v) The method explored for abrasion resistance measurements is in need of improvement, although some promising steps have been made.

4. ROTOR NOISE RESEARCH

4.1 General Objectives

In contrast to the other two fields, there has been a considerable amount of research in the noise field and much of it can be applied to ACV's. For example, well established rules are available for quietening pilot or passenger cabins, jet noise is reasonably well understood, and much can be done to alleviate noise generated by reciprocating type prime movers. The decision to use this knowledge is largely a question of economics and access to appropriate design competence. However the predominant noise sources from an ACV are usually the thrust system if it is aerodynamically propelled, or it can even be from lift fan intakes for other applications. Yet this is where research has not made the strides comparable to other areas; and this is no doubt due in part to the tendency until recently of the aerospace field to concentrate on the pure jet. A detailed programme of investigation of rotor generated noise to be undertaken in the facility described in Sect. 1 has therefore been selected as our primary objective.

As an important first step some exterior noise measurements on a typical ACV have been completed and are described here. Although they were primarily intended to aid us in defining research problems, they have proved interesting in their own right.

4.2 Some Propeller Noise Measurements

Noise measurements were for one propeller of Bell Voyageur, which is three bladed and 9 ft diameter. The measurements were made 100 ft from the propeller and on a line lying in its plane. The rotational speed was 34.36 Hz or 2061 rpm and tip speed 971 fps. Three techniques were used:

(i) on-line analogue using a standard sweep frequency analyzer,

(ii) off-line analogue using a lock-in amplifier technique,

(iii) digital analysis to obtain both the periodic and broad band noise components.

The on-line analogue technique used a Bruel and Kjaer 2107 which has a sweep range of 20 Hz to 20 KHz and uses a 6% bandwidth filter. The output was recorded on a type 2305 level recorder from the same maker. The major limitations of this technique is that pure tones beyond about the sixth harmonic are indistinguishable from the broad band noise. Also the rms meter used in this instrument was strictly only correct for pure tones or random noise, whereas propeller noise contains many harmonics as well as broad band noise.

In the lock-in amplifier technique, the major limitations of the sweep frequency analyzer are removed. The taped propeller noise signal is slowly swept with a puretone source and the beat signals so obtained can be processed to produce the rms contribution to the noise spectrum for the neighbourhood of this amplifier frequency. In effect the technique acts as a very narrow bandwidth filter, of width at most a few Hz. The difficulty with this technique is that it is extremely tedious since the tape has to be repetitively processed for all of the frequencies in the range of interest. Also the signals from the noise source are required to be stationary for relatively long time periods.

The third technique, digital processing, required the propeller noise signal to be recorded on magnetic tape which is compatible with a digital computer. A signal identifying the rotational rate of the propeller was simultaneously recorded on a second track of the same tape. A microphone calibration signal using a piston phone (250 Hz pure tone, of 124 dB intensity) was also recorded before and after the noise in order to calibrate the tape. The three analogue signals, namely the calibration signal, the propeller noise signal and the tachometer signal are then digitized. Prior to digitizing the signals two criteria were considered. One is that the sampling rate should be above the frequencies of acoustical interest in order to prevent "aliasing"*. Further, to assure that no signal of any significant strength exists beyond the sampling frequency, the noise signal was passed through a low-pass filter which was set such that at the sampling frequency, the signal was effectively zero compared to its strength, say one octave below this.

The digitized noise signal was then analyzed to extract information regarding its two basic components, namely, pure tones and broadband noise. The pure tones are attributable directly to the rotating pressure field surrounding each blade while the broadband noise is essentially due to the shedding of vortices from the blade tip and their subsequent breakup and mixing.

To obtain the pure tones, the tachometer signal, suitably processed to give a square wave, was used to establish the beginning and end of each shaft revolution on the taped noise signal. This allowed us to take an arithmetic average over a large number of complete cycles of the noise and arrive at an average signal of exactly one cycle duration. The averaged signal was then Fourier analyzed. The results of this analysis are shown in Figures 4.1a and 4.1b. It is seen that those for 100 cycle and 300 cycle averages are very nearly the same. The harmonic content of the noise reduces in intensity gradually, and beyond the 15th harmonic it is virtually nonexistent.

The broadband noise content can be evaluated by directly applying the Fourier transform to the digitized noise signal. The data for 8 time records each 0.8192 secs long (8192 points) was analyzed using the Hanning Window (Ref. 13) to correct for finite record length effects, and the eight frequency spectra were then averaged to produce the power spectral density curve shown in Figure 4.2. The harmonics corresponding to the blade passing frequency can be clearly seen above the broadband noise associated with vortex generation up to about the 13th at 1237 Hz, while the broadband noise continues to 5 KHz virtually undiminished.

The magnitudes of the harmonics associated with the blade passing frequency as obtained by the three methods are given in Figure 4.3, and there is reasonably good agreement.

4.3 Discussion and Conclusions

Trillo (Ref.6, pp.191-197) has discussed propeller noise quite extensively and notes the discrepancy between measured values and theoretical estimates. Apart from the questionable accuracy of the methods for estimation of the broadband noise, Trillo points out that there is a significant difference between the theoretical values of the harmonics calculated according to the method of Gutin (Ref. 17) and the observed values. Those quoted by Trillo decay much more slowly with increase in harmonic number. No explanation was given for this.

* Aliasing is an error which can occur as a direct result of digitizing. The problem is that when sampling at regular intervals higher frequencies can sometimes be mistaken for lower frequencies. To avoid this, the sampling frequency should be at least twice the highest frequency of interest.

In the present results, the decay with harmonic number was also found to be considerably slower than the theoretical rate, which has been shown in Figure 4.1 as a chain dotted line; the theoretical values were normalized with respect to the fundamental. One feature of the UTIAS results which does not appear to have been noted in ACV related literature is the presence of components at the shaft frequency and its harmonics. This implies that single propeller blade signatures are contributing to the noise, which in turn suggests that there are unsteady or nonuniform inflow effects. If such effects were present they would also occur in the blade frequency harmonics. An estimate of the "dirty inflow" effect was made by adding the noise components of the harmonics for both experimental and theoretical spectra, the increase when A - weighted was about 4 dB.

In general these results point to the need for carefully controlled experiments of the type planned for the rotor noise facility discussed in Section 1.

5. ACKNOWLEDGEMENTS

The research reviewed in this paper is the result of the efforts of many people and it is not possible to name them all here. The studies of cushion dynamics was undertaken under the direction of the author, while the materials work, and the noise measurements were directed respectively by Drs. R. C. Tennyson and G. W. Johnston of the UTIAS faculty. The funds for the equipment and operation have been provided by the National Research Council of Canada.

6. REFERENCES

1) Dau, K. Etkin, B. Surry, D. — "Aerodynamics of a Rectangular Wing with a Peripheral Jet for Air Cushion Takeoff and Landing". Report 65-59, September 1962, AFFDL, Wright-Patterson AFB, Ohio.

2) Sridhar, K. — "An Experimental Investigation of the Flow in and Behind Two Dimensional Jet Sheets Bounding a Cavity". UTIAS Report No. 94, August 1963.

3) Etkin, B. — Dynamics of Flight: Stability and Control, Wiley & Sons, New York, 1959.

4) Liiva, J. — "A Facility for Dynamic Testing of Airborne Models with Ground Effect". UTIAS Tech. Note No. 53, October 1961.

5) Kurylowich, G. — "The Determination of Aerodynamic Characteristics of Airborne Vehicles in Ground Effect Using Self Propelled Models". UTIAS Report No. 110, September 1965.

6) Trillo, R. — Marine Hovercraft Technology, International Textbook Company, London 1971.

7) Fowler, H. S. — "The Caspar ACV Research Projects, Report No. 1, Programme & Basic Data". National Research Council of Canada, Associate Committee on Air Cushion Technology, Report No. 3, March 1974.

8) Buckley, W. R. — "Determination of the Mechanical Properties of Coated Fabrics". Presented at the Conference of Stresses and Strains in Textile Structures. Shirley Institute, Manchester, England, September 1973.

9) Alley, V. L. Faison, R. W. — "Decelerator Fabric Constants Required by the Generalized Form of Hooke's Law". Journal of Aircraft, Vol. 9, No. 3, March 1973, pp.211-216.

10) — "Standard Methods for Testing Coated Fabrics". Designation D751-73, American Society for Testing and Materials, April 1973.

11) Sowerby, C. I. — "Abrasion Study of Coated Fabrics". Bachelors Thesis, Engineering Science Dept, University of Toronto, April, 1974.

12) Tennyson, R. C. — Private Communication.

13) Blackman, R. B. Tukey, A. J. — The Measurement of Power Spectra, Dover, New York, 1958.

14) Eggleton, P. L. Laframboise, J. E. — Field Evaluation of Towed Air Cushion Rafts. Transportation Development Agency, Ministry of Transport, Canada. Report No. TDA-500-166, January 1974.

15) Sullivan, P. A. and Placek, R. — A Review of the Status of Air Cushion Technology, UTIAS Review No. 33, May 1971.

16) Rubinstein, M. — "An Investigation of the Lift Generated by Plenum Chambers", UTIAS Tech. Note. (to be published)

17) Gutin, L. — "On the Sound Field of a Rotating Propeller". NACA T. N. 1195 (1948).



FIG. 1.1: THE CUSHION DYNAMICS FACILITY SHOWING AN 8 ft x 4 ft 325 lb. MULTICELL SKIRT UNDERGOING A STATIC ROLL TEST. THE DYNAMIC INSTRUMENTATION INCLUDES FORCE CELLS, DISPLACEMENT TRANSDUCERS AND A U/V CHART RECORDER

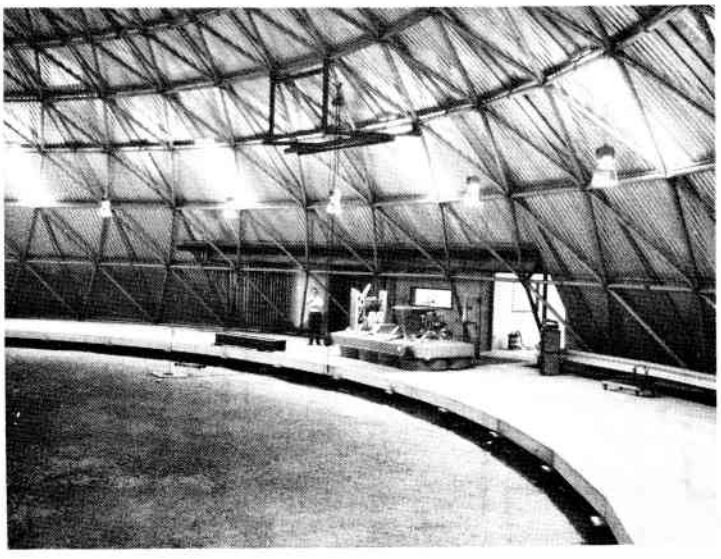


FIG. 1.2: INTERIOR VIEW OF THE ENCLOSED 140 ft DIAMETER CIRCULAR TRACK FACILITY LOOKING TOWARDS CONTROL ROOM. THE FIRST TEST VEHICLE, VAMPIRE 1 CAN BE SEEN AT THE ENTRANCE OF THE MODEL BAY

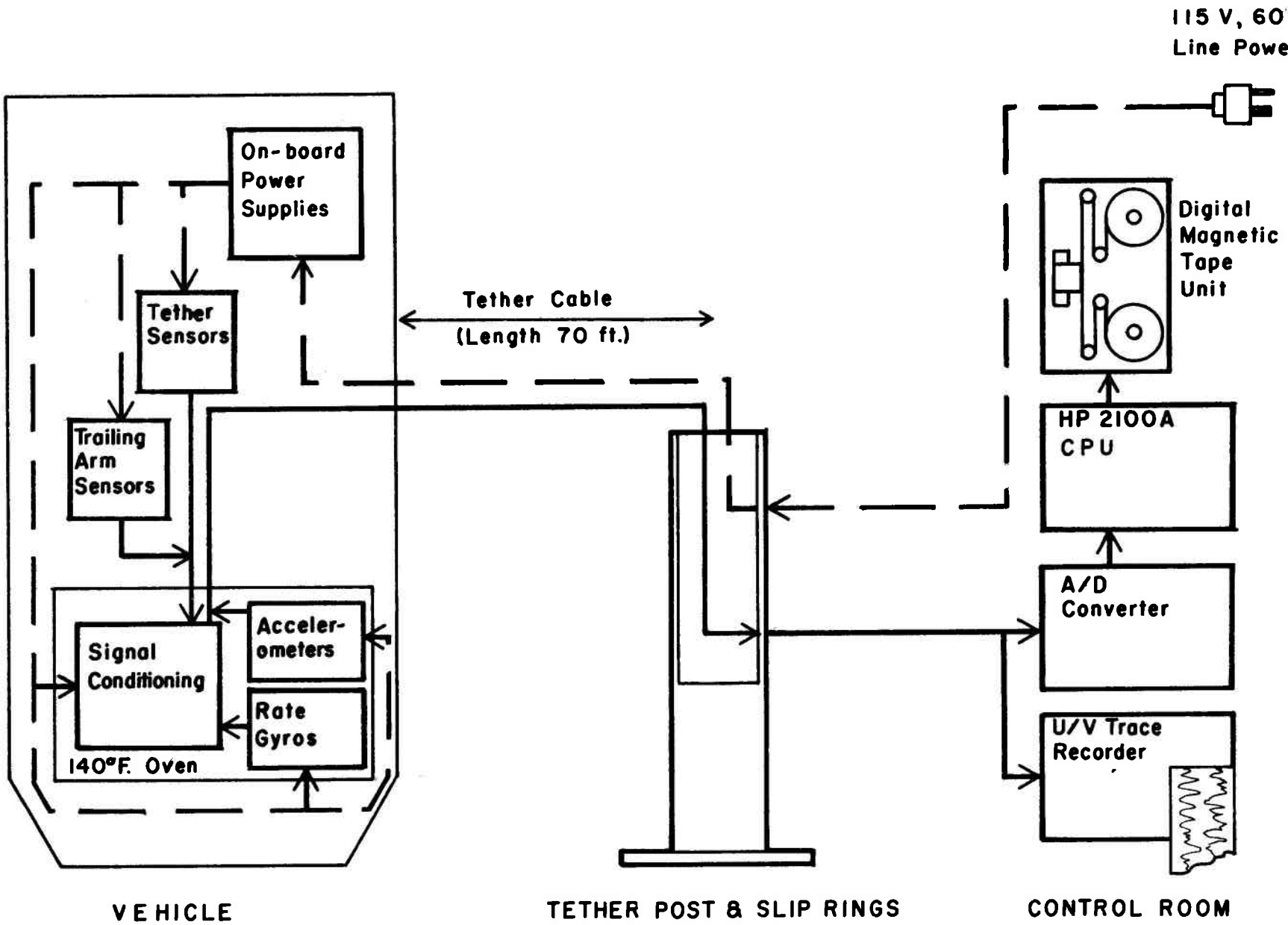


FIG. 1.3 CIRCULAR TRACK INSTRUMENTATION AND DATA ACQUISITION SYSTEM

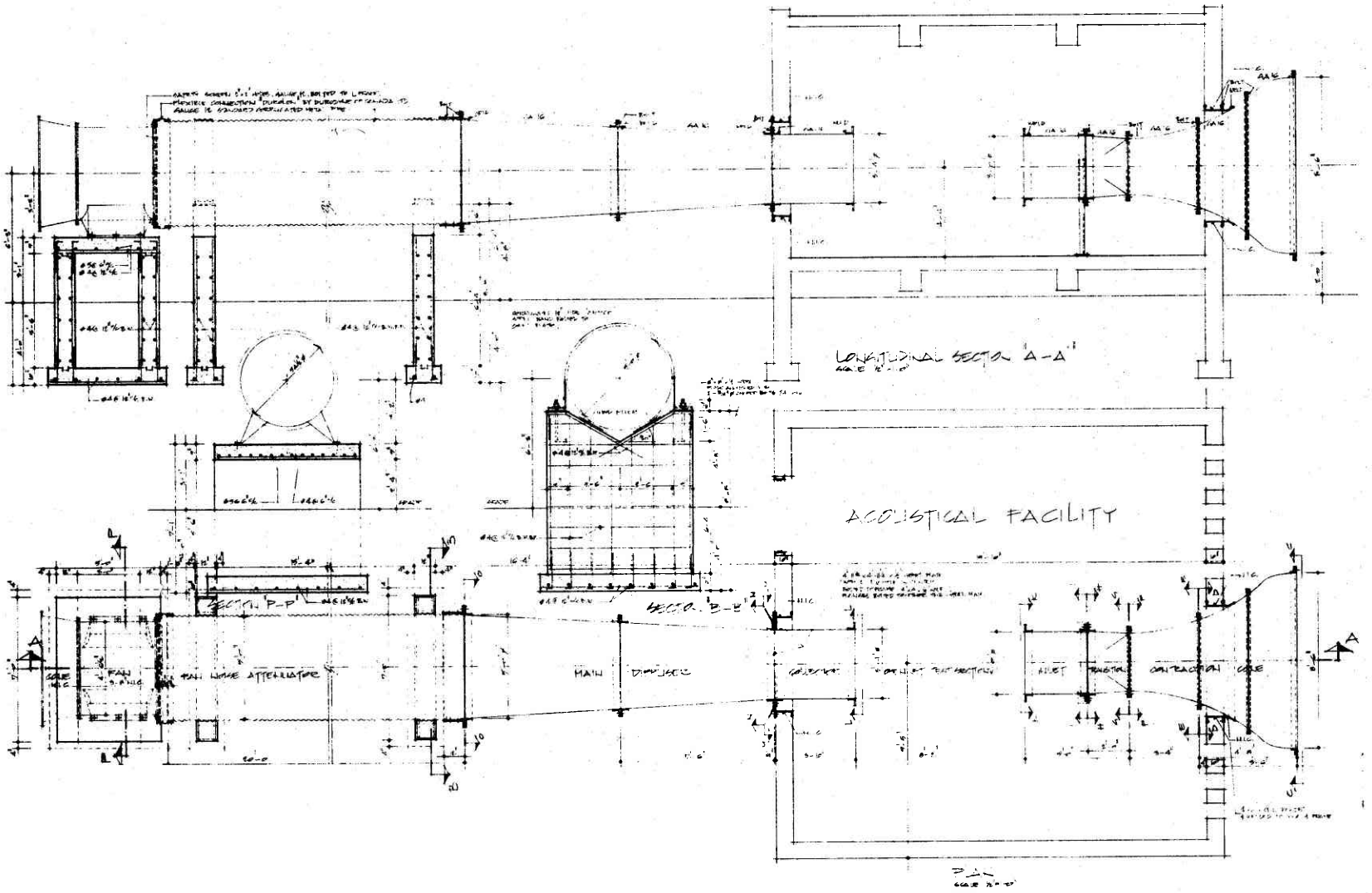


FIG. 1.4: ACOUSTIC TEST FACILITY

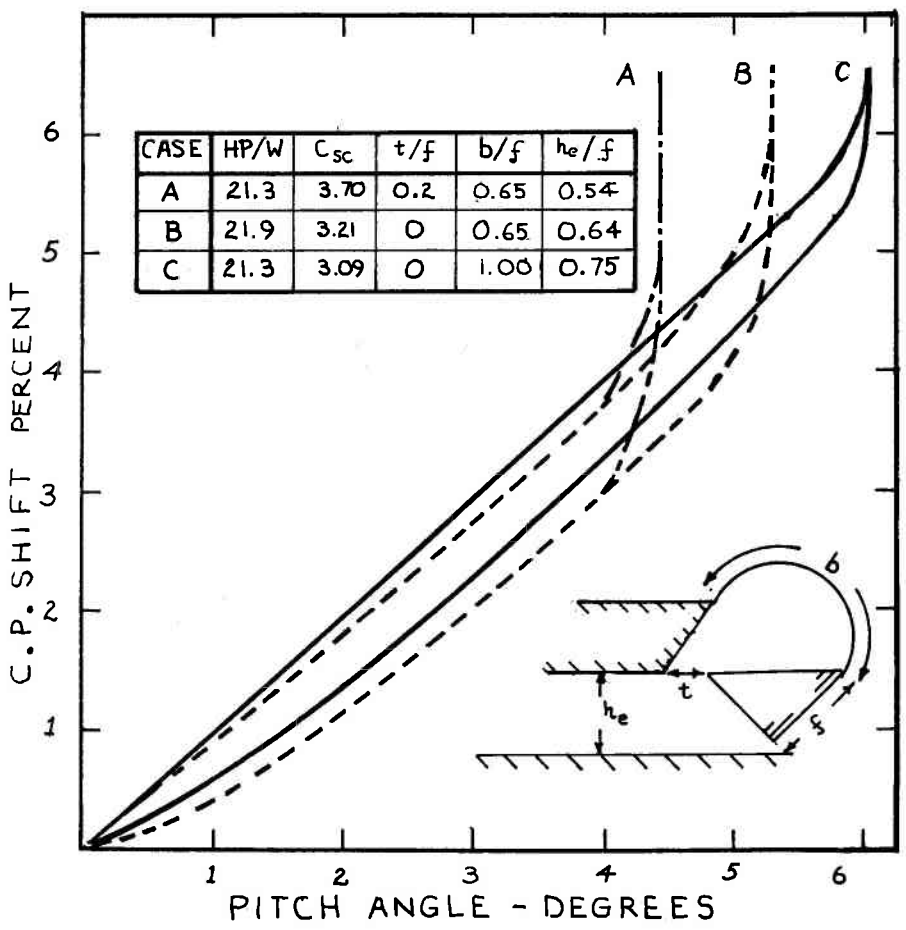


FIG. 2.1: EFFECT OF GEOMETRY CHANGES ON LOOP - FINGER SKIRT PITCH CHARACTERISTIC

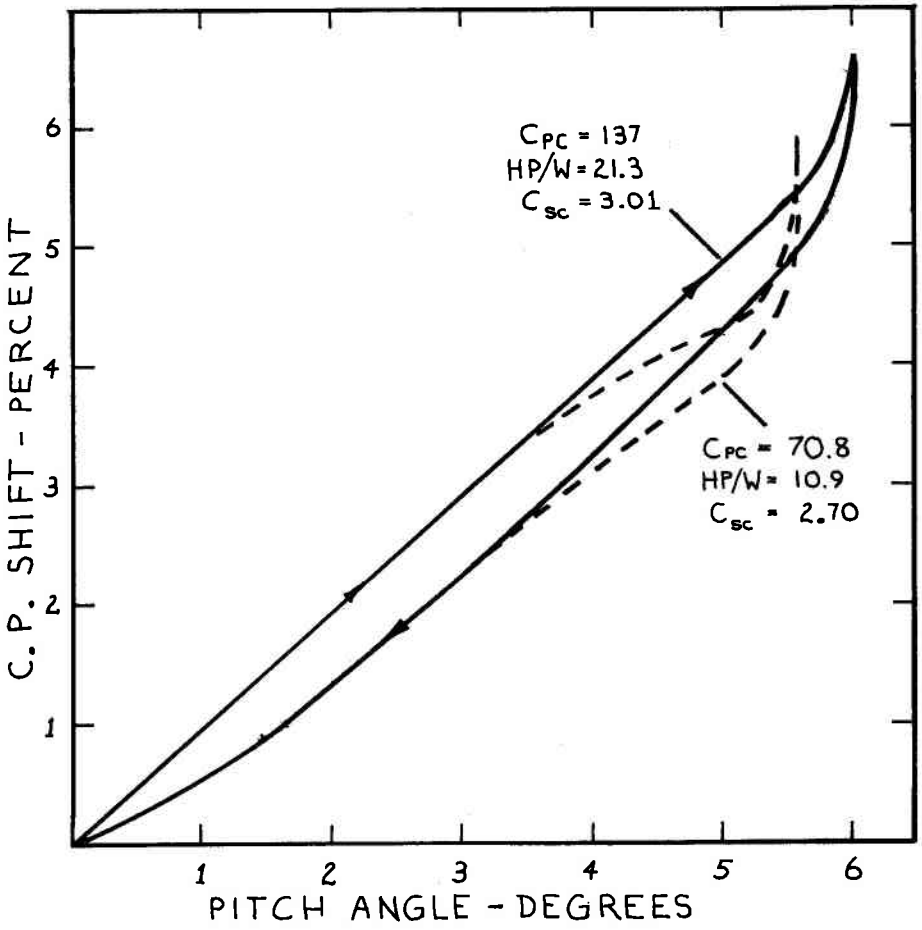


FIG. 2.2: EFFECT OF POWER INCREASE ON LOOP-FINGER SKIRT PITCH CHARACTERISTIC

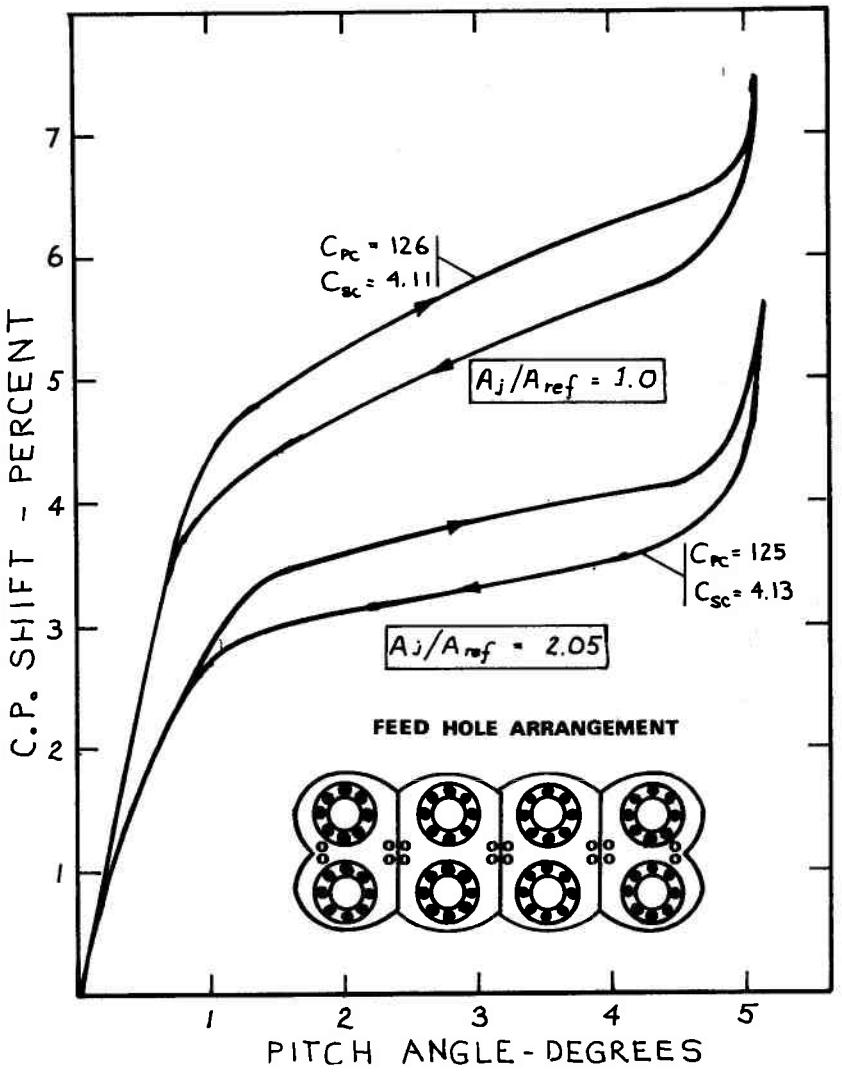


FIG. 2.3: TYPICAL RESULTS OF A MULTICELL TEST, SHOWING EFFECT OF VARIATION OF REGULATING HOLE SIZE

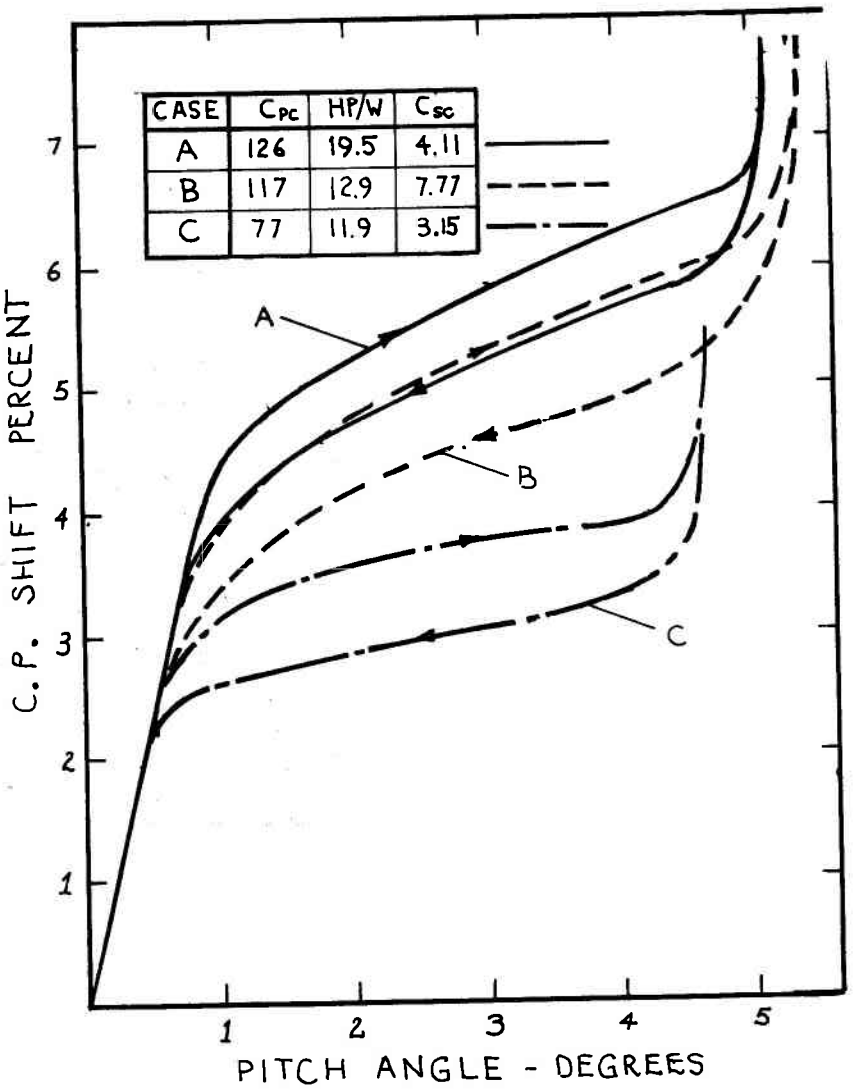


FIG. 2.4: EFFECT OF VARIATION OF C_{PC} AND C_{SC} ON A MULTICELL SKIRT

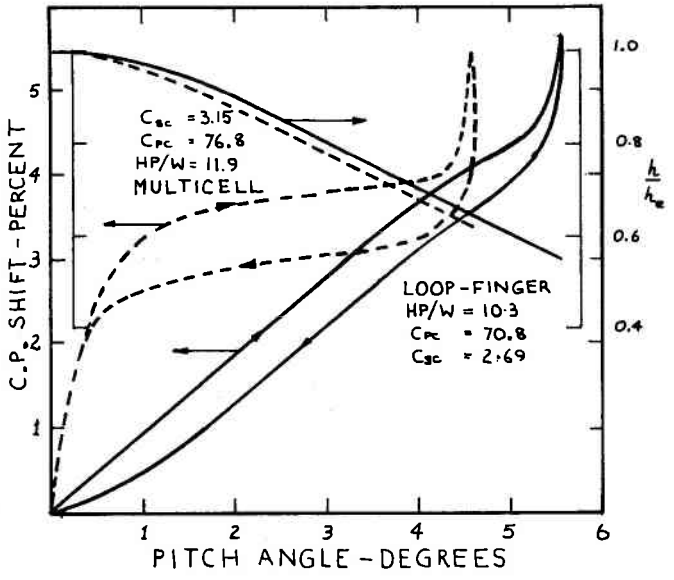


FIG. 2.5: COMPARISON OF LOOP-FINGER AND MULTICELL SKIRT FOR SIMILAR VALUES OF C_{PC} AND C_{SC}

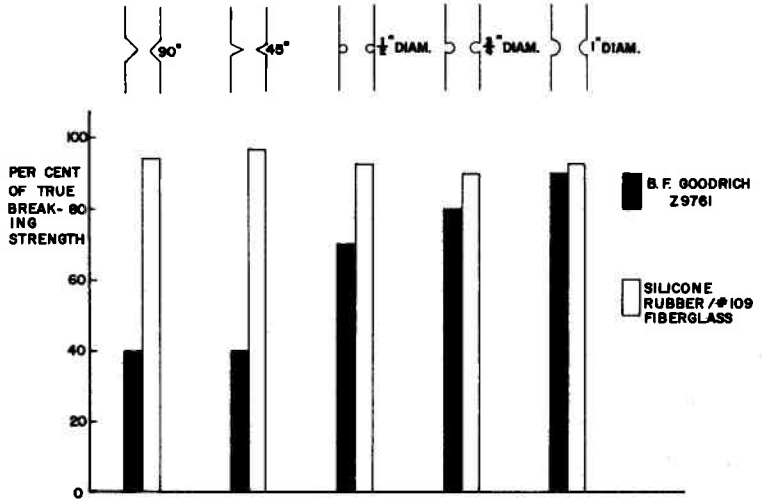


FIG. 3.1: EFFECT OF NOTCHES ON TENSILE STRENGTH

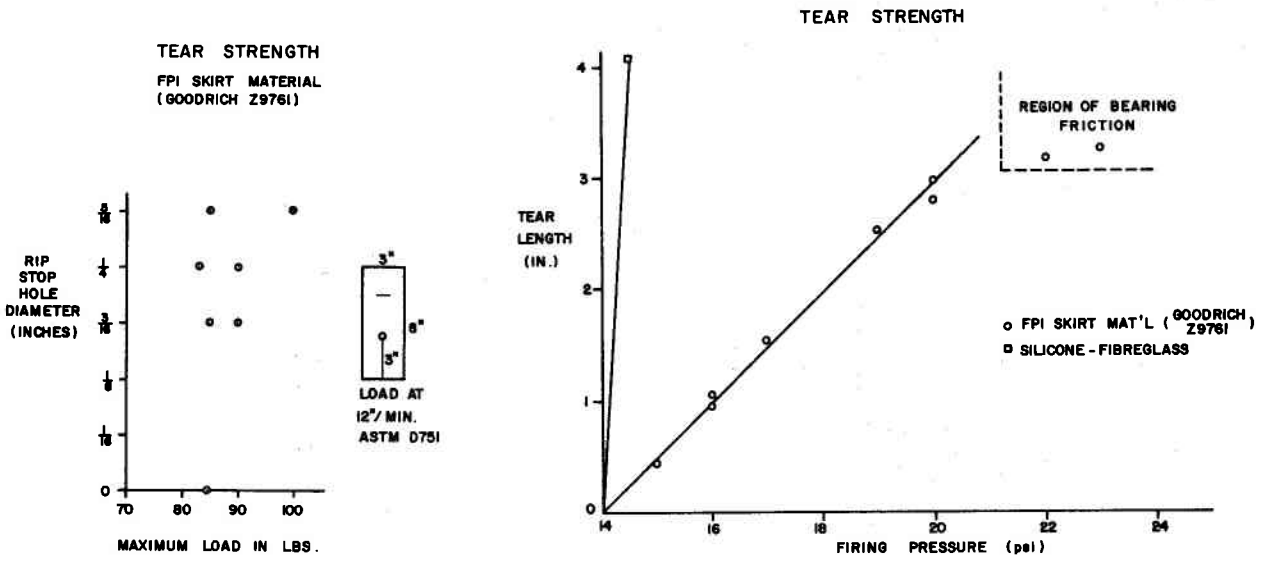


FIG. 3.2: COMPARISON OF TWO TEAR STRENGTH TESTS. THE SCATTER OF THE STANDARD ASTM D751 IS POOR COMPARED TO THAT OF THE GAS DRIVEN KNIFE TEST

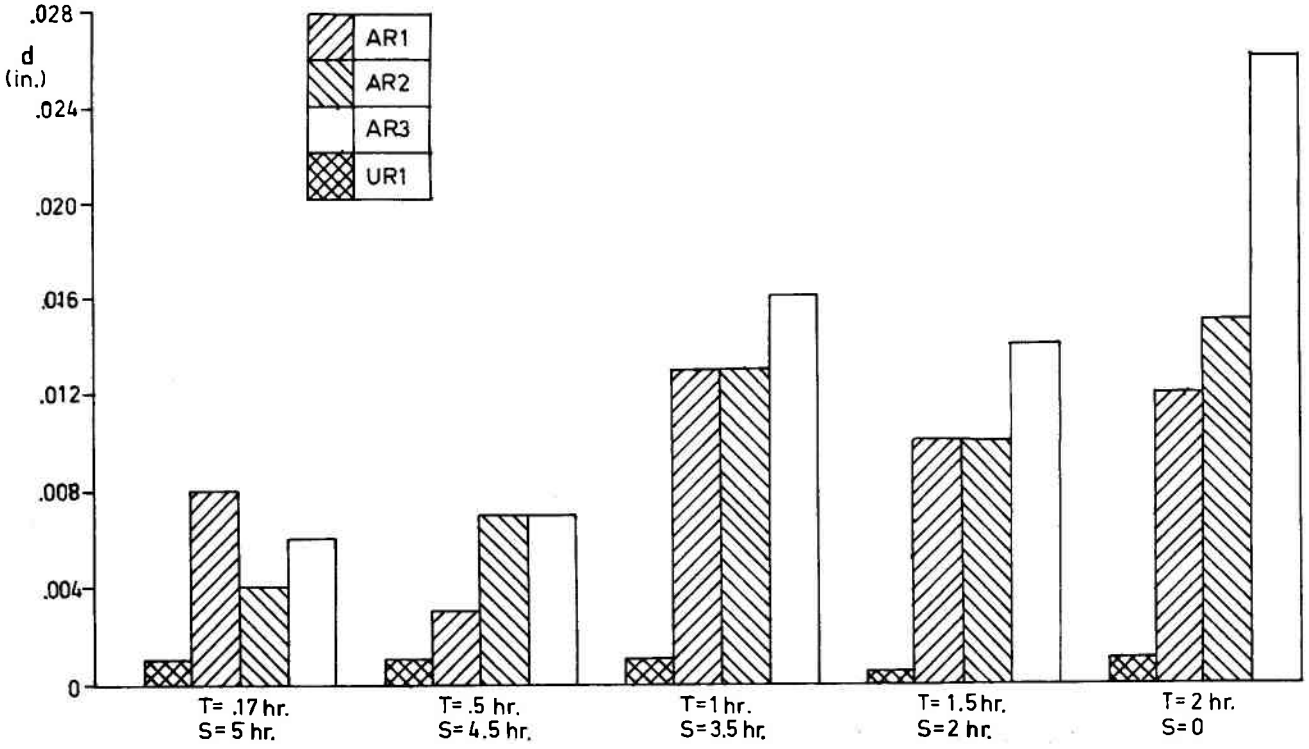


FIG. 3.3: COMPARATIVE ABRASION RESISTANCE OF FOUR SKIRT MATERIALS IN PRACTICAL USE

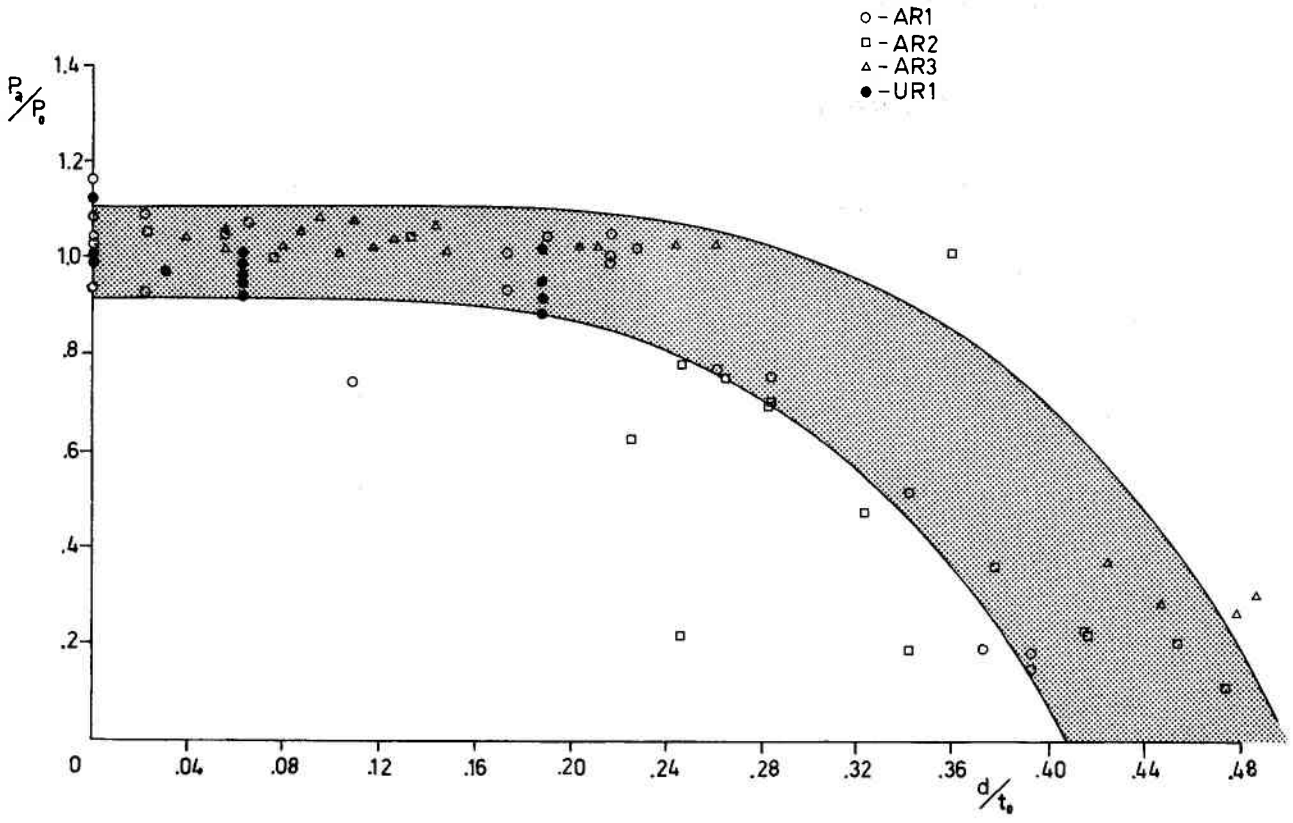


FIG. 3.4: EFFECT OF ABRASION ON MATERIAL STRENGTH

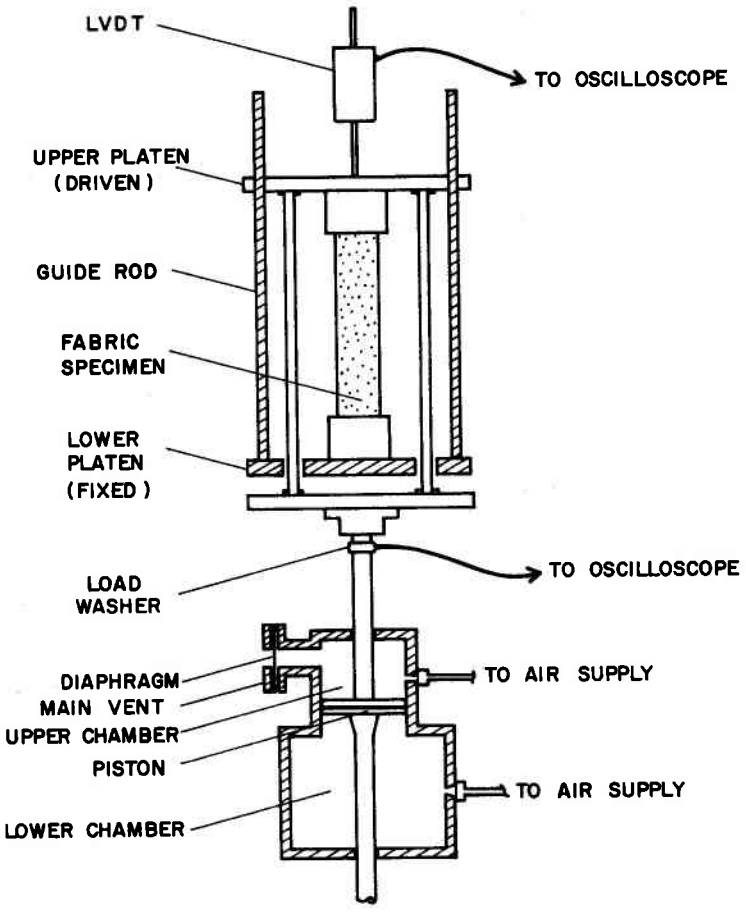


FIG. 3.5: VARIABLE STRAIN RATE TEST RIG

DYNAMIC TENSILE PROPERTIES - MAJOR AXIS

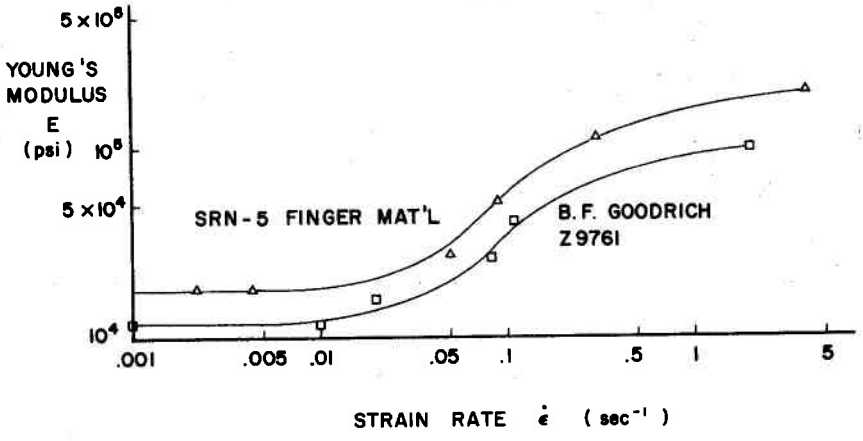


FIG. 3.6: SOME DYNAMIC TENSILE PROPERTIES FOR TYPICAL ACV SKIRT MATERIALS

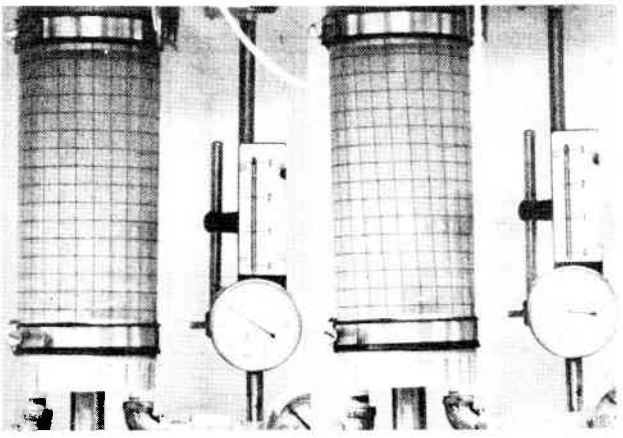


FIG. 3.7: TYPICAL CYLINDRICAL SPECIMENS IN UNLOADED AND LOADED STATES

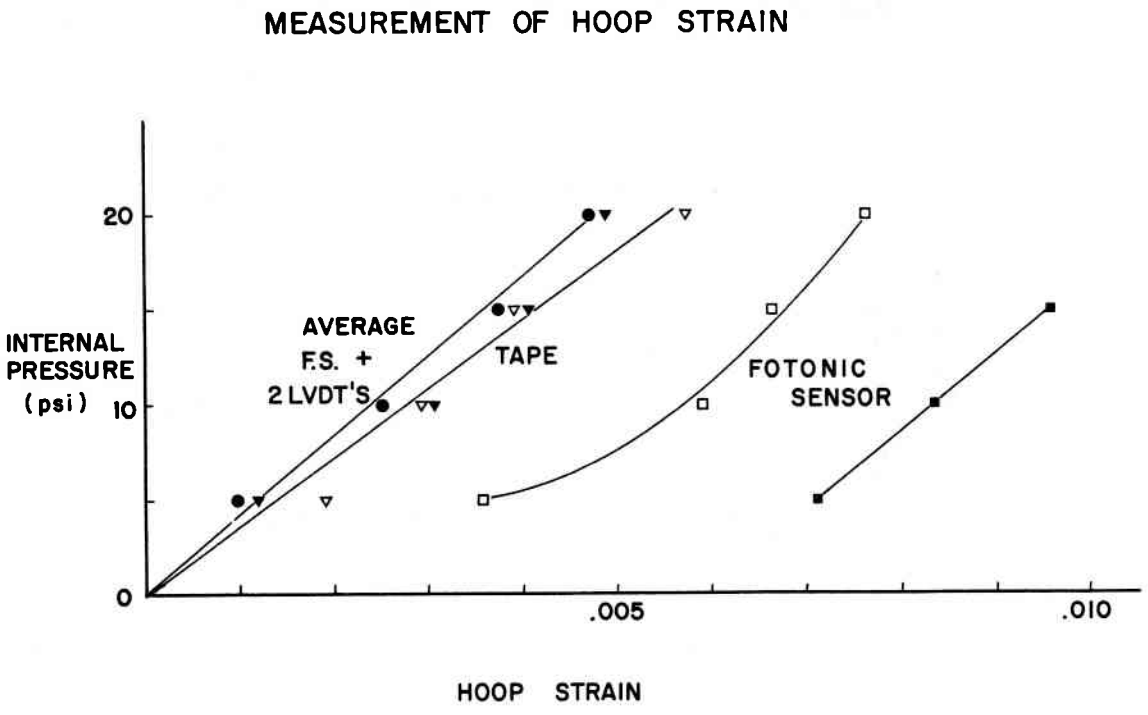


FIG. 3.8: DISCREPANCIES IN THE MEASUREMENT OF HOOP STRAIN

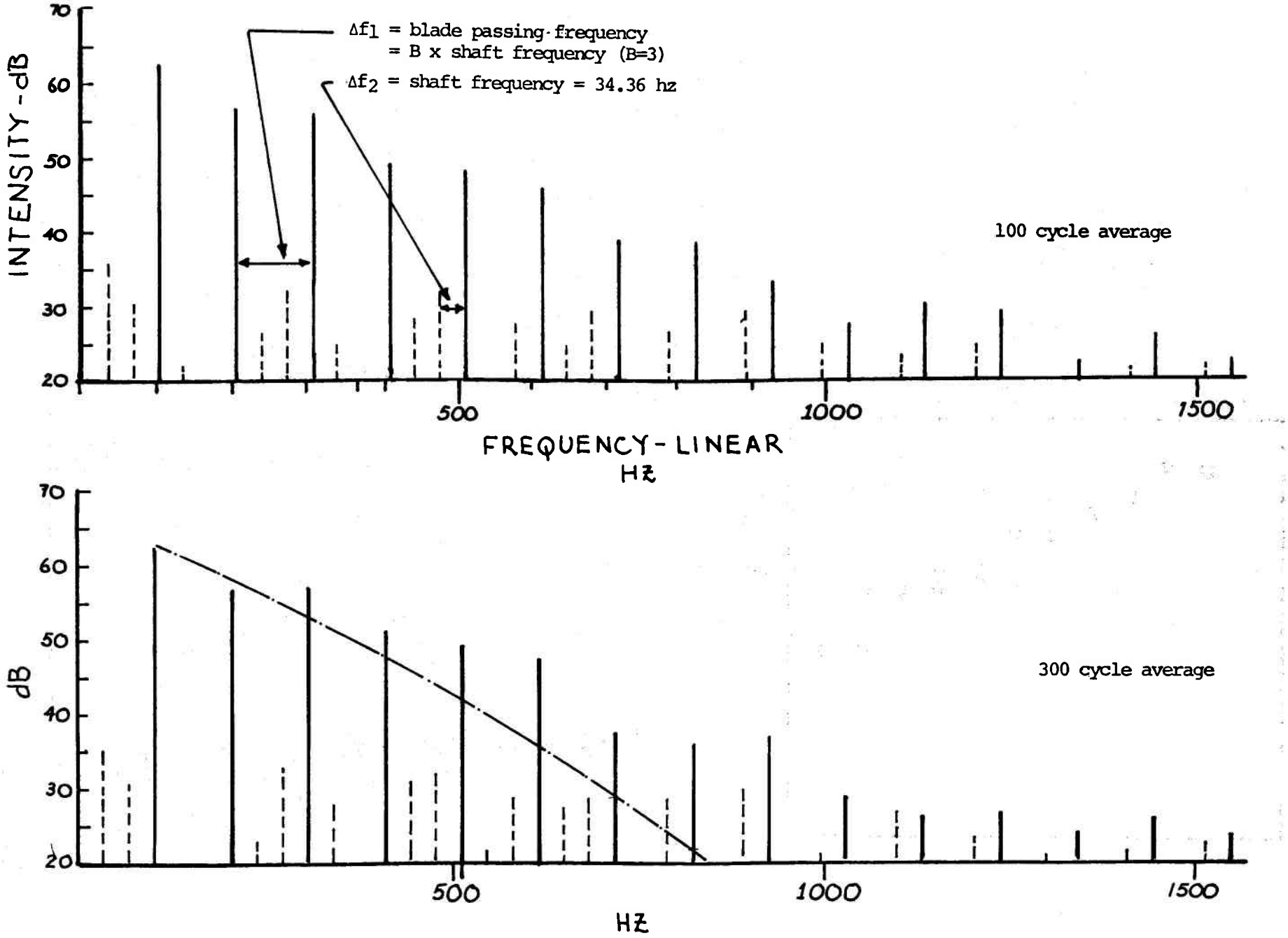


FIG. 4.1: PERIODIC NOISE SPECTRUM OF AN ACV PROPELLER
BOTH 100 AND 300 CYCLE AVERAGES GIVEN

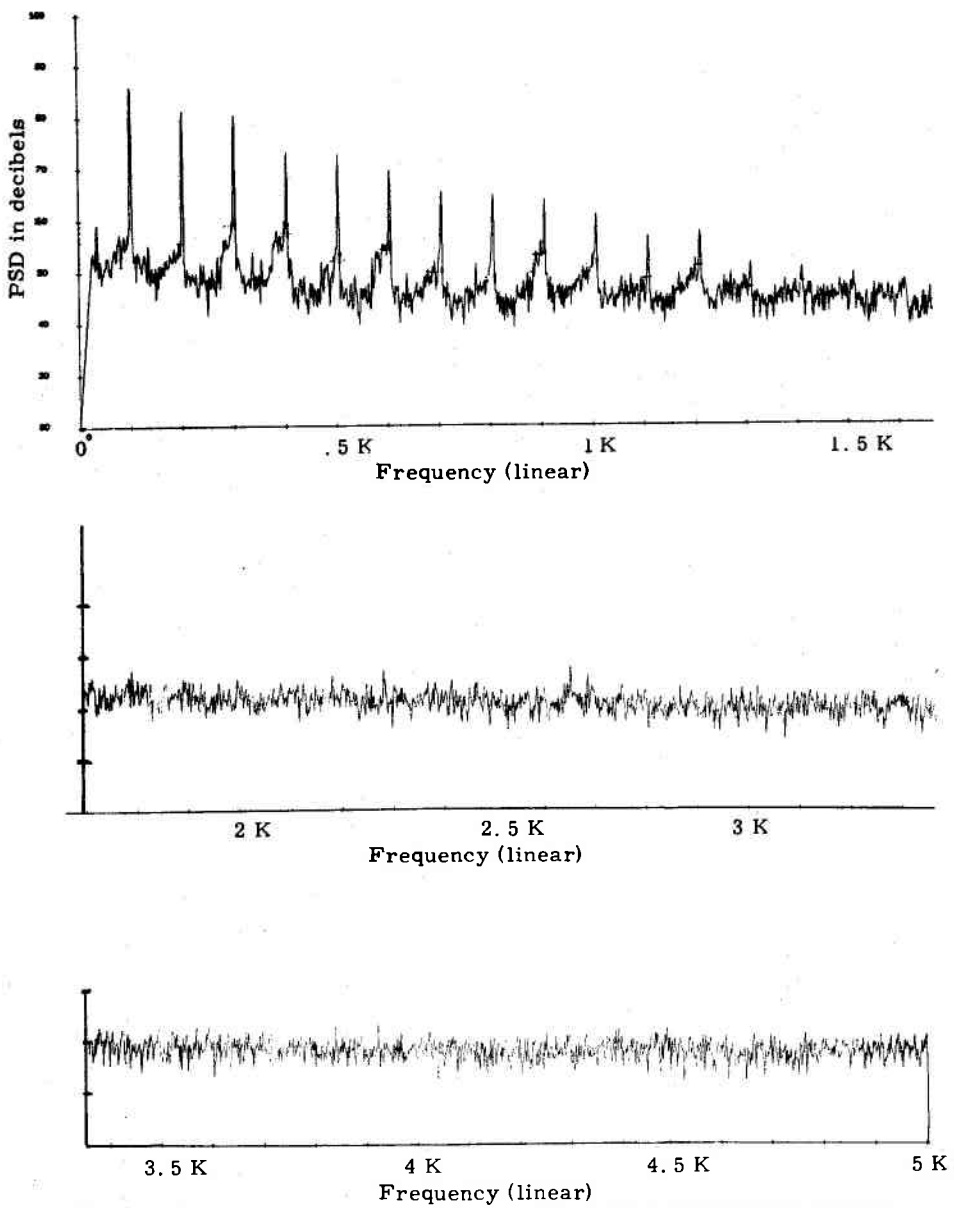


FIG. 4.2: POWER SPECTRAL DENSITY OF PROPELLER NOISE AVERAGED OVER EIGHT TIME RECORDS. BANDWIDTH = 1.2 Hz., 8192 POINT TRANSFORM.

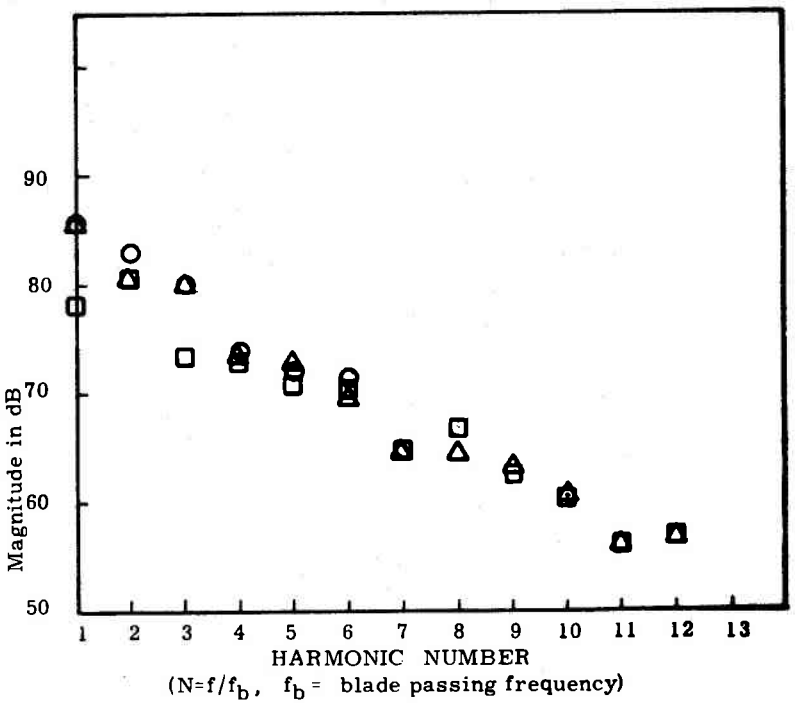


FIG. 4.3: Harmonic Analysis of Propeller Noise.

○ 6% Bandwidth Analysis
□ Lock-in Amplifier Technique
△ Digital Analysis